

## Polymeric fullerene chains in $\text{RbC}_{60}$ and $\text{KC}_{60}$

Ashfia Huq<sup>a,\*</sup>, P.W. Stephens<sup>a</sup>, Goetz M. Bendele<sup>a</sup>, R.M. Ibberson<sup>b</sup>

<sup>a</sup> State University of New York at Stony Brook, Stony Brook, NY 11794, USA

<sup>b</sup> ISIS Science Division, Rutherford Appleton Laboratory, Chilton Didcot, Oxfordshire OX11 0QX, UK

Received 27 June 2001; in final form 27 July 2001

### Abstract

We present a detailed study of the structure of the polymer phase of  $\text{AC}_{60}$  ( $A = \text{K}, \text{Rb}$ ) using data obtained from high-resolution neutron powder diffraction. We are able to obtain stable Rietveld refinements of both structures with no constraints on any carbon atom.  $\text{KC}_{60}$  has lattice parameters  $a = 9.952 \text{ \AA}$ ,  $b = 9.091 \text{ \AA}$ ,  $c = 14.372 \text{ \AA}$  in space group  $Pnmm$  and  $\text{RbC}_{60}$  has  $a = 10.125 \text{ \AA}$ ,  $b = 9.086 \text{ \AA}$ ,  $c = 14.207 \text{ \AA}$  and  $\beta = 90.316^\circ$  in space group  $I12/m1$ . We notice significant distortion throughout the ball from its original icosahedral symmetry. Coordinates of the atoms will allow more accurate theoretical calculation of the physical properties of these fullerides and might shed light on the differences among the cations and the dimensionality of their electronic properties. © 2001 Published by Elsevier Science B.V.

The physics of the one-dimensionally polymerized  $\text{AC}_{60}$  ( $A = \text{K}, \text{Rb}, \text{Cs}$ ) phase is very exciting and not completely understood, with significant differences among the cations [1]. All three have a structure consisting of chains of fullerenes linked by [2+2] cycloaddition, but their physical properties show subtle differences [1]. One of the most important unresolved questions concerning the polymer phase of  $\text{AC}_{60}$ , is the dimensionality of its electronic properties.  $\text{RbC}_{60}$  was originally argued to have a 1D electronic structure based on the electron spin resonance relaxation rate and the proximity of fullerenes along the polymerization direction [2]. The transition of  $\text{RbC}_{60}$  and  $\text{CsC}_{60}$  (but not  $\text{KC}_{60}$ ) to a magnetically ordered insulating phase below 50 and 40 K, respectively, [1] also argues for a 1D

electronic structure in those materials but raises the question, why  $\text{KC}_{60}$  is different. Magic angle spinning NMR measurement finds that the inter-chain interactions are different for the  $\text{KC}_{60}$  on one hand and  $\text{RbC}_{60}$  and  $\text{CsC}_{60}$  on the other [3] which may be the reason for their different transport properties. However, more recent NMR experiment carried out finds strong evidence for 3D electronic properties for  $\text{CsC}_{60}$  [4] in agreement with previous theoretical works [5,6]. In order to reconcile the issue it is crucial to attain a better picture of the structure to enable realistic models of these polymers.

Since the physical properties of fullerides have been shown to have very direct correlation to their structural properties, the difference of dimensionality of the electronic properties may be related to different orientation of the polymeric chains they form [5]. In an X-ray diffraction study Launois et al. [7] reported that the  $\text{RbC}_{60}$  is monoclinic instead of the originally claimed orthorhombic and

\* Corresponding author.

E-mail address: ashfia.huq@sunysb.edu (A. Huq).

confirmed the orthorhombic symmetry of  $\text{KC}_{60}$ . These results were based on the absence of diffuse scattering, and of the reflections for which  $h + k + l$  is odd in X-ray precession photographs of mosaic ( $\sim 2^\circ$  and  $2.5^\circ$ ) crystals of  $\text{RbC}_{60}$ . However, they were not able to refine the atomic coordinates and no lattice parameters were presented. They also did not detect a deviation of  $\beta$  from  $90^\circ$  in the monoclinic setting, which must be very small based on that, and previous X-ray work [8]. A previous neutron powder diffraction study [9] confirms the orthorhombic structure of  $\text{KC}_{60}$ , but did not report testing the monoclinic hypothesis. In this Letter we present a detailed neutron powder diffraction study of the structure of both  $\text{KC}_{60}$  and  $\text{RbC}_{60}$ .

Previous X-ray experiments on  $\text{CsC}_{60}$  [10],  $\text{RbC}_{60}$  and  $\text{KC}_{60}$  [8] gave C–C bond lengths at the cyclo-addition site considerably larger than those accepted by theory [11]. The accuracy with which atomic positions can be measured using X-ray diffraction is limited by a few factors. The X-ray scattering cross-section of C is small compared to the intercalants and moreover, the intensity at high  $Q$  (small  $d$  spacing) is further reduced by atomic form factor. In order to measure distances with accuracy on the order of the expected spread of distances (i.e.,  $\sim 1.39$  Å for double bonds and 1.45 Å for single bonds to  $\text{sp}^2$  carbons and 1.65 Å for  $\text{sp}^3$  carbons) one needs to be able to acquire good diffraction pattern at  $d$ -spacing less than 1 Å. In all of the previous experiments (X-ray and neutron) the distances between the  $\text{sp}^2$  C atoms were fixed to the expected value and only the bridgehead carbon positions were allowed to refine. In contrast with all previous neutron and X-ray work we refine the position of every atom, and are able to attain stable results without restraining any lengths or angles.

Samples were prepared by solid-state reaction of commercially available high purity Rb or K metal and sublimed high purity  $\text{C}_{60}$  powder. The sealed Pyrex tube was heated between 200 and 500 °C for more than one month with intermediate grinding and adjustment of ratio in response to X-ray measurements to achieve stoichiometry  $\text{AC}_{60}$  as precisely as possible. Preliminary X-ray powder patterns led us to conclude that both samples were

chemically and structurally single-phase polymer<sup>1</sup>. Approximately 2 g of material was used for all measurements.

Neutron powder diffraction data of both samples' polymer phase were collected at the high resolution powder diffractometer (HRPD) at Beamline S8 at the ISIS spallation neutron source at Rutherford Appleton Laboratory. Three banks of ZnS scintillation detectors were used to record the detected neutron intensities in the backscattering ( $160 < 2\theta < 176$ ),  $90^\circ$  ( $87^\circ < 2\theta < 93^\circ$ ) and low angle position ( $28^\circ < 2\theta < 32^\circ$ ) as a function of time of flight. Neutron patterns between 16 and 24 h were recorded for  $\text{RbC}_{60}$  at  $T = 5, 100$  and 200 K and for  $\text{KC}_{60}$  at room temperature. The diffraction pattern for  $\text{RbC}_{60}$  was recorded at room temperature for 8 h. For the  $\text{KC}_{60}$  sample diffraction measurement was also made at the high-resolution powder diffractometer BT1, at the NIST Center for Neutron Research. There, diffracted intensity was measured as a function of detector angle at a wavelength of 1.5 Å at  $T = 6$  K ( $\sim 40$  h).

Our results obtained from this experiment are summarized as follows. The structure of  $\text{RbC}_{60}$  is monoclinic with lattice parameters  $a = 10.125$  Å,  $b = 9.086$  Å,  $c = 14.207$  Å and  $\beta = 90.316^\circ$  at room temperature. The plane of the [2+2] linkage is oriented at an angle  $\psi = 46^\circ$  about its  $b$  axis from the  $bc$  plane and all parallel fullerene chains share the same orientation angle.  $\text{KC}_{60}$  on the other hand is orthorhombic as originally suggested [8] with lattice parameters  $a = 9.952$  Å,  $b = 9.091$  Å,  $c = 14.372$  Å at room temperature. The orientation angle of the chain passing through the origin is  $\psi = 50^\circ$  from the  $bc$  plane and that passing through the center of the unit cell is  $-\psi$ . The inter ( $r$ ) and intra ( $r'$ ) fullerene bond lengths between  $\text{sp}^3$  bonding carbons are found to be 1.6 and 1.55 Å

<sup>1</sup>  $\text{RbC}_{60}$  transforms directly from the rock salt to the polymer phase, and so the best samples were obtained by cooling from 200 °C to room temperature continuously at the rate of 1 °C per hour. The polymer phase of  $\text{KC}_{60}$  is stable at room temperature, but disproportionates in a range of temperature between room temperature and the rock salt phase and so we obtained the best sample of polymeric  $\text{KC}_{60}$  by quenching into  $\text{LN}_2$  and warming to room temperature in ice water.

for  $\text{KC}_{60}$  and both are 1.55 Å for  $\text{RbC}_{60}$ . The single and double bonds are generally grouped around the theoretically predicted values of 1.39 and 1.45 Å (see Table 1).

We now discuss the details of analysis that led to the previously stated conclusions. In the case of these phases the most plausible orthorhombic space groups that accommodate the molecular symmetry of polymeric  $\text{C}_{60}$  are  $Pnmm$  and  $Immm$  (which can be either ordered or disordered). It is possible to carry out refinement of a powder pattern using only the lattice and profile parameters to describe the position and shape of all Bragg peaks letting the intensity of each peak vary freely, commonly known as a LeBail fit [12]. Since it does not use any atomic information it is often the most decisive way to determine a space group or distinguish between two space groups. However, for  $\text{RbC}_{60}$  all efforts to obtain a satisfactory LeBail fit for an orthorhombic unit cell failed and hence a monoclinic setting was considered (inset of Fig. 1). Based on previous work done on this phase we know that if the bonding mechanism of the  $\text{C}_{60}$  is [2+2] cycloaddition then the bonding direction must be a 2-fold symmetry axis, therefore the monoclinic  $b$  axis. Also there should be a fullerene located at the center of the cell in addition to the one at the origin and the origin must be an inversion center. The only monoclinic space group which satisfies these criteria is  $I2/m$ . It should also

be mentioned that the number of Bragg reflections over the range of  $d$ -spacing of interest remains approximately the same when the symmetry is lowered from orthorhombic  $Pnmm$  to monoclinic  $I2/m$ . Having found the correct unit cell and space group the crystal structure was refined. The previously published coordinates [8] provided a reasonable starting point for the least square fitting program GSAS [13]. The background was treated to be a cosine series with 20 refined coefficients. The Bragg peaks were fitted with an exponential pseudo-voigt convolution function that takes into account anisotropic line-shape broadening [14] a frequently observed phenomenon in powder diffraction patterns. The coordinates of all the carbons could be simultaneously refined in a stable refinement, illustrated in Fig. 1.

In the case of  $\text{KC}_{60}$  it was not possible to determine the lattice and space group unambiguously from just a Le Bail fit. However, some peaks were observed which were better fitted with a space group that allows  $h + k + l = \text{odd}$  reflections as suggested by the results published by Launois [7]. Three space groups were considered while doing a Rietveld refinement (Fig. 2). For the body-centered space group  $Immm$  both ordered and disordered configurations were considered. In this model the best Rietveld fit is obtained if the chain orientation  $\psi = 49^\circ$  with  $R_{\text{wp}} = 4.69$  and  $\chi^2 = 4.8$ . The space group  $Pnmm$  structure has glide planes

Table 1

Lattice parameters and thermal parameters for both  $\text{KC}_{60}$  and  $\text{RbC}_{60}$  at various temperatures with  $F = 0$  (no constraint).  $U_{11}$ ,  $U_{22}$  etc. are the anisotropic thermal parameters for the cation

Temperature (K)	$\text{RbC}_{60}$ (ISIS)				$\text{KC}_{60}$ (NIST)	$\text{KC}_{60}$ (ISIS)
	5	100	200	300	6	300
Space group	$I12/m1$				$Pnmm$	
<i>Lattice parameters</i>						
$a$	10.0843 (03)	10.0995 (03)	10.1137 (03)	10.1257 (03)	9.9010 (21)	9.9525 (09)
$b$	9.0887 (01)	9.0893 (01)	9.0886 (01)	9.0865 (01)	9.1185 (18)	9.0917 (08)
$c$	14.1583 (03)	14.1693 (03)	14.1879 (04)	14.2070 (04)	14.3467 (32)	14.3740 (12)
$\beta$	90.375 (02)	90.359 (02)	90.341 (02)	90.317 (02)		
$\chi^2$	4.349	3.329	3.64	1.473	0.5069	2.058
$R_{\text{wp}}$	1.47	1.44	1.32	3.36	5.63	3.0
<i>Thermal parameters</i>						
Uiso:C	0.000922	0.00209	0.0017	0.00261	0.02096	0.00189
$U_{11}$ , $U_{22}$	0.00194 (Uiso)	0.00, 0.10749	0.0078, 0.1742	0.003, 0.2224	0.0900, 0.4000	0.09, 0.19048
$U_{33}$ , $U_{13}$		0.00633, -0.0073	0.00120, -0.01352	0.02179, 0.0168	0.2054	0.4000

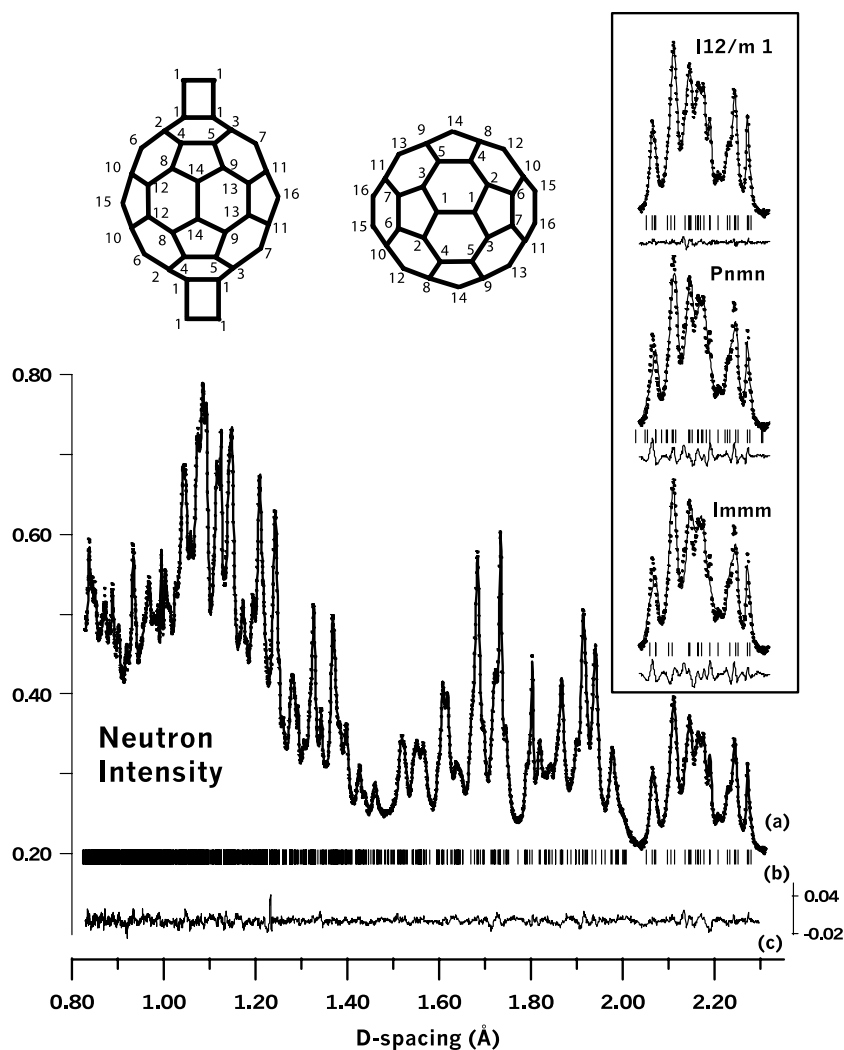


Fig. 1. Neutron diffraction pattern of  $\text{RbC}_{60}$  at  $T = 200$  K. This Rietveld fit has a weighted  $R_{\text{wp}}$  factor of 1.32% and  $\chi^2 = 3.64$ . The inset shows the LeBail fits of the three probable space groups over the range of  $d$  spacing 2.04 to 2.32 Å. Trace (a) is the raw data and best fit profile, (b) indicates peak positions of  $\text{RbC}_{60}$  and (c) is the difference between observed and calculated intensities. Two  $\text{C}_{60}$  balls are shown for the labels of the carbon atoms.

and so the fullerenes at  $(0, 0, 0)$  and  $(1/2, 1/2, 1/2)$  are rotated in the opposite direction. We obtain a significantly better fit to the data for this crystallographic description of the unit cell with  $R_{\text{wp}} = 3.0$  and  $\chi^2 = 2.058$ . The orientation of chain is found to be  $\psi = 50^\circ$ . A grid search was carried out for the orientation angle from  $\psi = 0^\circ$  to  $90^\circ$  with a  $2^\circ$  interval to avoid any bias of the chain orientation. It is not possible to detect a shift of  $\beta$

from  $90^\circ$  in  $I 2/m$  setting and the fit is considerably worse with  $R_{\text{wp}} = 5.35$  and  $\chi^2 = 5.58$ .

In both cases, the fullerene symmetry is reduced from its original icosahedral point group to having  $2/m$  symmetry. Due to this reduction in symmetry there is no mirror plane containing the chain axis so that the atoms 2 and 3, 4 and 5, etc. (Fig. 1) are not equivalent. This was also noted in an NMR experiment on  $\text{CsC}_{60}$  [4] where it was found that

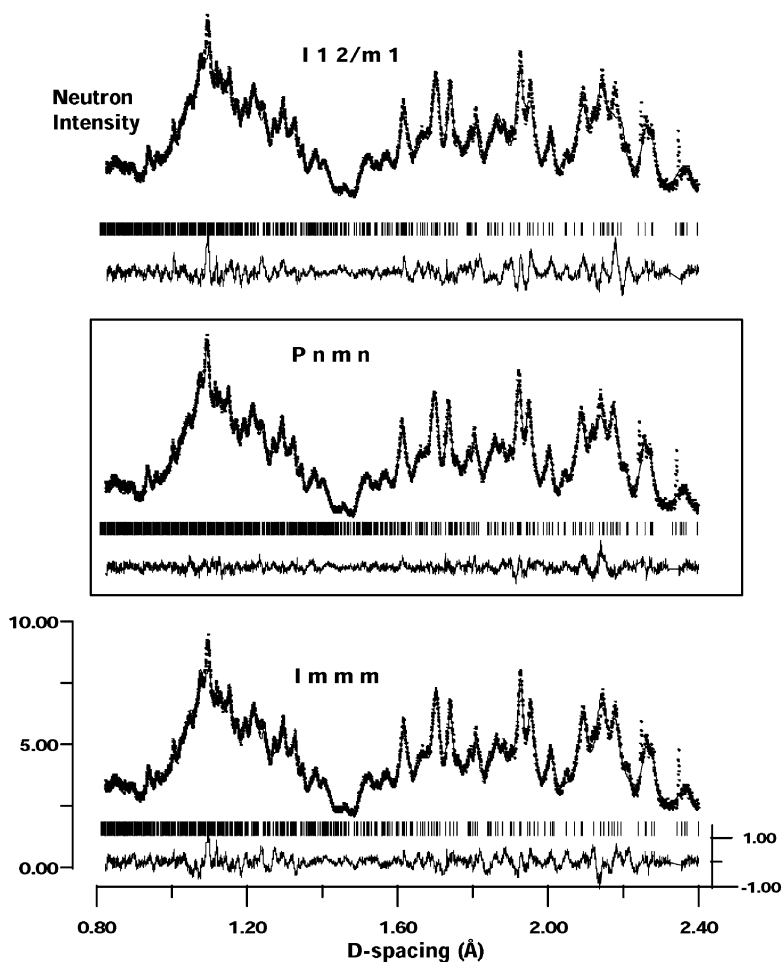


Fig. 2. Rietveld fit of the likely space group candidates for  $KC_{60}$ . The  $R_{wp}$  factor and  $\chi^2$  for the space groups  $I m m m$ ,  $P n m n$  and  $I 1 2/m 1$  are (4.69, 3.0, 5.35) and (4.8, 2.21, 5.58), respectively.

the environment surrounding crystal sites 2 and 3 are not identical.

The ability to obtain stable refinement of all structural parameters with reasonable inter-atomic distances, bond angles, positive Debye–Waller factors, etc., is generally accepted as strong evidence that the proposed structure is correct. However, it is of interest to consider the accuracy of the result. It is widely accepted that the statistical estimated standard deviation from Rietveld refinement, listed in Table 2, drastically underestimates the accurate error bounds of the structural results. Often chemical knowledge of

certain molecules gives us a good reference point to ascertain the reliability of the model. Once a suitable starting model is found, the Rietveld method allows the simultaneous refinement of structural parameters such as atomic positions, site occupancies and Debye–Waller factors along with lattice and profile parameters. In GSAS it is also possible to provide a set of inter-atomic distances along with standard deviations i.e., enforce some soft constraints on how much the atom positions can change. The reduced  $\chi^2$  or ‘goodness of fit’ is defined by the minimization function

Table 2  
 Fractional coordinates and the distance of each C atom from the origin at the center of the ball ( $d_o$ ), from the nearest cation ( $d_c$ ) and pyramidalization angle ( $\theta_p$ ) for both  $KC_{60}$  and  $RbC_{60}$ . The numbers in the parenthesis are the estimated standard deviations obtained from Rietveld refinements

$KC_{60}$ (ISIS)												
$T = 300$ K												
Fractional coordinates												
	x	y	z	$d_c$	$d_o$	$\theta_p$	x	y	z	$d_c$	$d_o$	$\theta_p$
C1	-0.0571 (05)	0.4167 (05)	0.0377 (03)	4.5774 (50)	3.8677 (46)	8.64 (67)	-0.0576 (06)	0.4123 (05)	0.0334 (04)	4.5003 (59)	3.8223 (46)	
C2	-0.0245 (04)	0.3370 (04)	0.1307 (03)	5.3730 (40)	3.5881 (38)	8.64 (67)	-0.0372 (05)	0.3380 (06)	0.1267 (04)	5.1678 (51)	3.5970 (55)	10.01 (86)
C3	-0.1838 (05)	0.3353 (04)	0.0074 (03)	3.5331 (48)	3.5706 (41)	8.53 (79)	-0.1872 (06)	0.3346 (06)	0.0037 (04)	3.4606 (59)	3.5647 (56)	9.09 (95)
C4	0.1036 (04)	0.2902 (04)	0.1520 (03)	4.9251 (42)	3.5686 (39)	11.90 (56)	0.0927 (06)	0.2868 (07)	0.1588 (04)	5.0391 (58)	3.5799 (61)	13.26 (82)
C5	-0.2115 (05)	0.2864 (04)	-0.0811 (03)	3.6832 (46)	3.5647 (43)	12.17 (56)	-0.2080 (06)	0.2838 (07)	-0.0856 (05)	3.7217 (62)	3.5308 (63)	10.41 (92)
C6	-0.1342 (04)	0.2582 (05)	0.1634 (03)	4.8976 (42)	3.5617 (44)	12.13 (58)	-0.1480 (05)	0.2594 (05)	0.1481 (04)	4.6478 (51)	3.5022 (51)	9.34 (92)
C7	-0.2345 (04)	0.2521 (04)	0.0880 (03)	3.7263 (39)	3.5211 (39)	9.75 (66)	-0.2478 (05)	0.2540 (07)	0.0746 (04)	3.5279 (56)	3.5455 (57)	10.92 (90)
C8	0.1219 (04)	0.1547 (04)	0.2102 (03)	4.5107 (41)	3.5255 (41)	10.60 (54)	0.1029 (06)	0.1511 (07)	0.2142 (05)	4.4478 (70)	3.5238 (70)	11.64 (73)
C9	-0.2880 (05)	0.1586 (04)	-0.0947 (03)	3.9994 (42)	3.5230 (47)	10.12 (58)	-0.2858 (06)	0.1567 (06)	-0.1071 (04)	4.0831 (56)	3.5341 (58)	13.38 (87)
C10	-0.1186 (05)	0.1276 (04)	0.2201 (03)	4.3145 (42)	3.5340 (43)	11.42 (58)	-0.1442 (07)	0.1337 (05)	0.2090 (04)	4.5948 (57)	3.5390 (58)	12.21 (73)
C11	-0.3199 (05)	0.1289 (04)	0.0764 (04)	3.9864 (41)	3.6024 (50)	14.51 (54)	-0.3325 (07)	0.1285 (07)	0.0554 (04)	3.8488 (65)	3.5958 (68)	14.47 (107)
C12	0.0132 (04)	0.0791 (04)	0.2445 (03)	3.6965 (42)	3.5465 (42)	12.00 (41)	-0.0200 (06)	0.0792 (05)	0.2408 (04)	3.8057 (57)	3.5341 (57)	11.68 (57)
C13	-0.3417 (04)	0.0807 (04)	-0.0190 (03)	4.1413 (37)	3.5452 (40)	11.38 (44)	-0.3401 (06)	0.0803 (06)	-0.0301 (05)	4.1562 (56)	3.4877 (60)	8.59 (147)
C14	0.2374 (04)	0.0752 (04)	0.1766 (03)	5.2107 (40)	3.5469 (41)	12.08 (32)	0.2212 (06)	0.0747 (06)	0.1819 (04)	5.0539 (58)	3.5414 (58)	10.58 (55)
C15	-0.2018 (07)	0	0.2039 (04)	4.6809 (55)	3.5306 (62)	12.10 (57)	-0.2354 (09)	0	0.1873 (05)	5.0729 (71)	3.5685 (80)	12.47 (72)
C16	-0.2939 (07)	0	0.1318 (05)	5.3421 (37)	3.5019 (71)	8.87 (82)	-0.3149 (10)	0	0.1161 (06)	5.1803 (45)	3.5535 (97)	10.28 (104)

$$\chi^2 = \frac{\sum_{i=1}^{N_{\text{obs}}} w_i (I_{\text{oi}} - I_{\text{ci}})^2 + F \sum_{j=1}^{M_{\text{cons}}} \frac{1}{\sigma_j^2} (d_{\text{oj}} - d_{\text{cj}})^2}{(N_{\text{obs}} - N_{\text{var}})}$$

Here  $w_i = 1/\sigma_i^2$ , is the statistical weight of the  $i$ th profile observation which is the inverse of the variance of the  $i$ th observation.  $I_{\text{oi}}$  and  $I_{\text{ci}}$  are observed and calculated intensities,  $d_{\text{oj}}$  and  $d_{\text{cj}}$  are the calculated and expected bond lengths and  $\sigma_j^2$  is the variance of the imposed constraints. The scaling factor  $F$  is used to adjust the contribution of these so-called ‘soft constraints’ to the total minimization factor. We started the refinement of atomic positions with no constraints and obtained stable refinements. Experience with aromatic molecules leads one to expect that between  $\text{sp}^2$  carbons, single bonds should be in the range  $1.45 \pm 0.01$  Å, double bonds in the range  $1.39 \pm 0.01$  Å, between  $\text{sp}^3$  carbons it should be  $1.6$  Å, and that between  $\text{sp}^2$  and  $\text{sp}^3$ ,  $1.5$  Å. Calculations and experiments on fullerenes give a range of  $1.43$ – $1.47$  Å for C–C bonds and  $1.36$ – $1.4$  Å for C=C bonds [15]. Choi and Kertesz [11] have considered various models for fullerene bonding and conclude that the  $\text{sp}^3$ – $\text{sp}^3$  bond should be in the neighborhood of  $1.6$

Å and the  $\text{sp}^2$ – $\text{sp}^3$  distance around  $1.5$  Å. However, the distances obtained from an unconstrained model for these polymers were not in complete agreement with these expected bond lengths. We progressively increased  $F$  to bias the distances toward their expected values and studied its influence of the quality of fit. The distances used for soft constraint are  $(d_{\text{cj}} \pm \sigma_j) = 1.39 \pm 0.02$  Å for double bonds (6:6 bonds),  $1.45 \pm 0.02$  Å for single bonds (6:5 bonds). The interfullerene and intrafullerene bond lengths  $r$  and  $r'$  were constrained to be  $1.6 \pm 0.05$  Å. Figs. 3 and 4 show the distribution of bond lengths for different values of  $F$  starting from having no constraint, i.e.,  $F = 0$  to  $10^4$  for  $\text{KC}_{60}$  and  $\text{RbC}_{60}$ , respectively. In both data sets we observe that the double and single bond lengths cluster around  $1.4$  and  $1.45$  Å. However, there is a significant spread in the distribution of these bond lengths, both for single and double bonds. As the constraints get more stringent, the bond lengths respond to the constraint rather than the diffraction data causing a clear segregation between single and double bonds. If  $F$  is increased from  $0$  (no constraint) to  $100$  we do not notice any appreciable

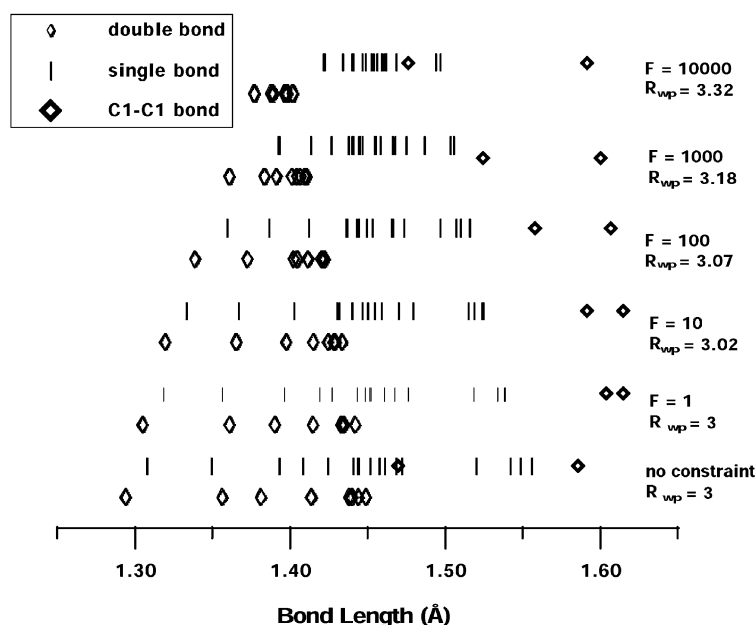


Fig. 3. Bond length distribution of  $\text{KC}_{60}$  at  $T = 300$  K as a function of  $F$ , where  $F$  describes the weight of the constraint (defined in the text). The constraint imposed on double bonds is  $1.39 \pm 0.02$  Å, on single bonds is  $1.45 \pm 0.02$  Å and that on  $\text{sp}^3$  bonds is  $1.6 \pm 0.05$  Å.

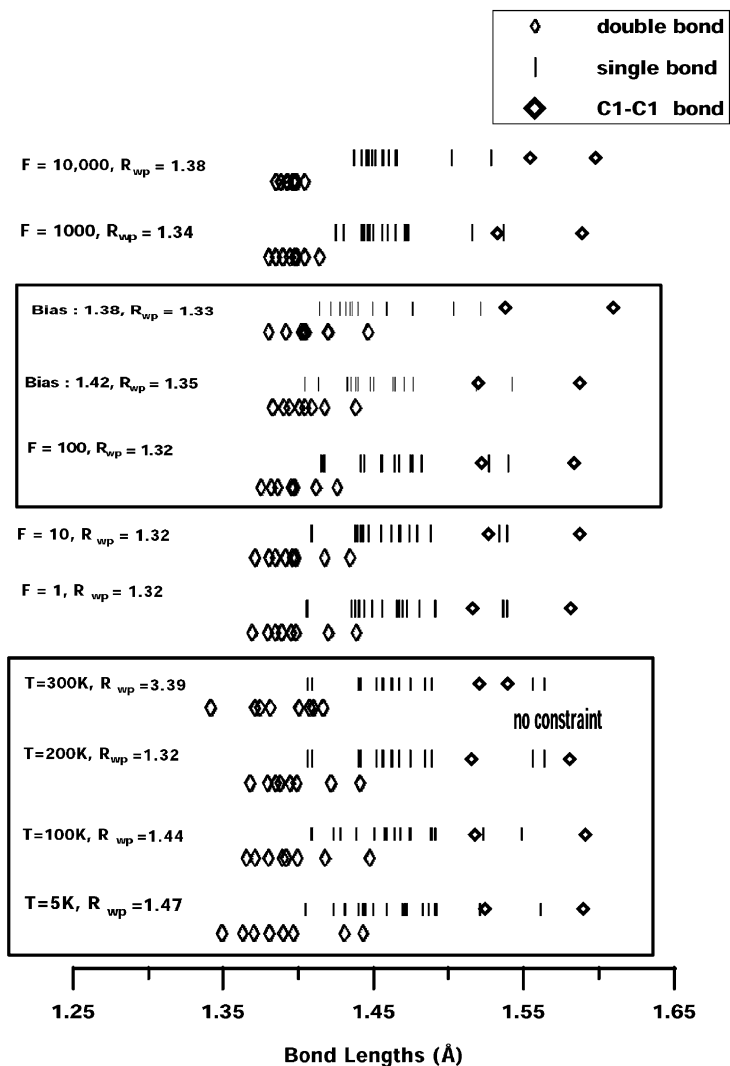


Fig. 4. Bond length distribution of  $\text{RbC}_{60}$  at  $T = 200$  K as a function of  $F$ . The first box from the top shows the bond lengths when the constraint imposed on all bond lengths are 1.38 and 1.42 for  $F = 100$ . The lower box shows the temperature dependence of the bond length with no constraints.

degradation of the fit in either set of data. However, by increasing the value of  $F$  beyond 100 we compromise the goodness of the fit to the diffraction data. In the case of  $\text{RbC}_{60}$  we also notice (upper box, Fig. 4) that if we try to bias all the bond lengths to either 1.38 or 1.42 Å we do not see any significant changes in the bond lengths. Lower box in Fig. 4 shows the bond length distribution obtained for  $\text{RbC}_{60}$  at different temperatures with

$F = 0$ . It should be mentioned that the order of the bonds is more or less the same for all these temperatures. That is to say the outliers from the mean value are the bonds between the same pairs of carbon atoms. The two ‘single’ bonds longer than 1.5 Å are connected to the bridgehead  $\text{sp}^3$  carbons (1–2 and 1–3) as expected for  $\text{sp}^2$ – $\text{sp}^3$  bonds. The C1–C1 interfullerene distance is 1.55 Å and the C1–C1 intrafullerene distance is 1.6 Å in agree-



ment with previous experimental and theoretical works.

For the  $\text{KC}_{60}$  data we do not have complete distinction between single and double bond lengths<sup>2</sup>. Also the quality of the  $\text{KC}_{60}$  sample is not as good as that of  $\text{RbC}_{60}$  which is clearly noticeable from the peak widths in the diffraction pattern. The data obtained for  $\text{KC}_{60}$  at 6 K also show that the single and double bond lengths converge to their expected values of 1.39 and 1.45 Å if  $F = 100$ .

From the histogram of bond lengths shown in Figs. 3 and 4 we notice that the buckyball in  $\text{KC}_{60}$  is significantly more distorted than  $\text{RbC}_{60}$ . One measure of deformation of the ball is given by the distance of each carbon atom on the ball from the center of the ball. These distances are listed in Table 2. In order to understand the stated distortion we tried to see if there is any correlation between the distorted bond lengths and the proximity of the carbon atoms to the nearest cation. Fig. 5 shows the distribution of bond lengths and groups the carbon atoms according to their distances from the closest cation. These distances, which are also listed in Table 2 show no obvious relation to the scatter of the bond lengths from their expected values. Excluding the  $\text{sp}^3$  carbons, we see that the distances are within 1.8% of the 3.55 Å radius of the undistorted, uncharged  $\text{C}_{60}$  molecule [16]. Ogitsu [17] found a somewhat smaller fullerene in their density functional theory analysis of  $\text{KC}_{60}$ , with a comparable (2%) elliptical distortion in the plane (radii from 3.41–3.49 Å). Another way to calculate the distortion of the ball is to calculate the pyramidalization angle [18] at each carbon position. In a free (undistorted)  $\text{C}_{60}$  this angle has a value of  $11.64^\circ$ . The values of these angles are also listed in Table 2. The statistical errors were propagated numerically from the uncertainties associated with the positions of the atoms obtained from GSAS; they therefore represent

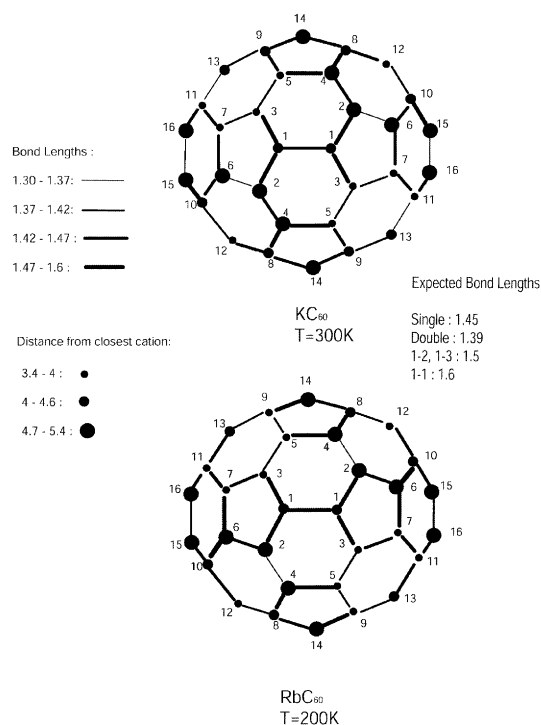


Fig. 5. View of the buckyball for both  $\text{KC}_{60}$  and  $\text{RbC}_{60}$  showing the variations of the bond lengths between carbon atoms and the distance of each carbon from the nearest cation.

statistical uncertainties rather than estimate of accuracy of the results. More careful theoretical calculations based on the observed coordinates and chain orientation will shed more light on the transport properties of these polymers.

## Acknowledgements

Research at SUNY was supported by US Department of Energy under the Grant No 6476789. Research carried out in part at SUNY X3 beamline at NSLS which is supported by the Division of Basic Energy Sciences of the US Department of Energy under Grant No DE-FG02-86ER45231. The authors would like to thank Brian Toby for the use of Beamline BT1 at the NIST Center for Neutron Research. Majority of the experiments were carried out at the High Resolution Powder Diffractometer (HRPD) at Beamline S8 at the ISIS

<sup>2</sup> Here we should point out that we excluded two regions ( $d$  spacing 2.238–2.246 and 2.321–2.346 Å) because of the presence of two very sharp peaks unlikely to be a part of the diffraction pattern of the sample. Hence the uncertainty associated with this data set is significantly larger than the  $\text{RbC}_{60}$  data set.

spallation neutron source at Rutherford Appleton Laboratory.

## References

- [1] F. Bommeli, L. Degiorgi, P. Wachter, O. Legeza, A. Janossy, G. Oszlanyi, O. Chauvet, L. Forro, *Phys. Rev. B* 51 (1995) 14794.
- [2] O. Chauvet, G. Oszlanyi, L. Forro, P.W. Stephens, M. Tegze, G. Faigel, A. Janossy, *Phys. Rev. Lett.* 72 (1994) 2721.
- [3] H. Alloul, V. Brouet, E. Lafontaine, L. Mailer, L. Forro, *Phys. Rev. Lett.* 76 (1996) 2922.
- [4] T.M. de Swiet, J.L. Yarger, T. Wagberg, J. Hone, B.J. Gross, M. Tomaselli, J.J. Titman, A. Zettl, M. Mehring, *Phys. Rev. Lett.* 84 (2000) 717.
- [5] K. Tanaka, T. Saito, Y. Oshima, T. Yamabe, H. Kobayashi, *Chem. Phys. Lett.* 272 (1997) 189.
- [6] S.C. Erwin, G.V. Krishna, E.J. Mele, *Phys. Rev. B* 51 (1995) 7345.
- [7] P. Launois, R. Moret, J. Hone, A. Zettl, *Phys. Rev. Lett.* 81 (1998) 4420.
- [8] P.W. Stephens, G. Bortel, G. Faigel, M. Tegze, A. Janossy, S. Pekker, G. Oszlanyi, L. Forro, *Nature* 370 (1994) 636.
- [9] H.M. Guerrero, R.L. Cappelletti, D.A. Neumann, T. Yildirim, *Chem. Phys. Lett.* 297 (1998) 265.
- [10] S. Rouziere, S. Margadonna, K. Prassides, A.N. Fitch, *Europhys. Lett.* 51 (2000) 314.
- [11] C.H. Choi, M. Kertesz, *Chem. Phys. Lett.* 282 (1998) 318.
- [12] A. Le Bail et al., *Mater. Res. Bull.* 23 (1988) 447.
- [13] A.C. Larson, R.B. Von Dreele, GSAS General Structure Analysis System Los Alamos Laboratory Report No. LA-UR-86-748, Los Alamos, 1987.
- [14] P.W. Stephens, *J. Appl. Crystallogr.* 32 (1999) 281.
- [15] G.E. Scuseria, in: W.E. Billups, A.M. Ciufolini (Eds.), *Buckminsterfullerenes*, VCH, Weinheim, 1993.
- [16] W.I.F. David, R.M. Ibberson, C. Matthewman, K. Prassides, J.S. Dennis, J.P. Hare, H.W. Kroto, R. Taylor, D.R.M. Walton, *Nature* 353 (1991) 147.
- [17] T. Ogitsu, T.M. Briere, K. Kusakabe, S. Tsuneyuki, Y. Tateyama, *Phys. Rev. B* 58 (1998) 13925.
- [18] R.C. Haddon, *J. Phys. Chem. A* 105 (2001) 4164.